Near-Surface Current Measurements in the Gulf Stream Using an Upward-Looking Acoustic Doppler Current Profiler

WILLIAM E. JOHNS

Rosenstiel School of Marine and Atmospheric Science, Division of Meteorology & Physical Oceanography, University of Miami, Miami, Florida

(Manuscript received 3 July 1987, in final form 2 December 1987)

ABSTRACT

During November 1986, a 6-day record was collected from a 150 kHz Acoustic Doppler Current Profiler (ADCP) mounted in the upward-looking mode on a subsurface mooring in the Gulf Stream near Cape Hatteras. The flotation unit used for the ADCP was a newly developed streamlined float, designed to minimize the effects of drag-induced tilt and high-frequency buoy motion on the range and precision of the Doppler measurements. The overall performance of the float was found to be excellent, with a mean tilt of less than 2° in up to 2 kt of current and a high apparent stability to vortex-induced oscillations. As a result, good velocity data were obtained to within 30 m of the surface from a mean depth of 375 m. A comparison of the near-field ADCP velocity data with a conventional Aanderaa current meter moored 20 m below the ADCP yielded mean and root-mean-square speed and direction differences of 1.0 ± 3.7 cm s^{-1} and $0.5 \pm 2.9°$, respectively. Also, a comparison with Pegasus velocity profiles taken within 1 n mi of the mooring site showed qualitatively good agreement, with the ADCP reproducing well the small-scale vertical structure. Significant fluctuations in the vertical component were also observed, related to diurnal migration of biological scatterers, with vertical "speeds" often in excess of 3–4 cm s^{-1}.

1. Introduction

One of the longstanding needs of the modern oceanographic research community has been a reliable, cost-efficient system for measuring near-surface currents in energetic regions of the ocean for long periods of time. In the past, methods for obtaining such data have generally relied upon shipboard-based hydrographic or free-drop measurements which, although useful, are impractical to carry out for extended durations or at sufficiently rapid intervals to capture the true synoptic variability of the flow being investigated. Problems with obtaining near-surface measurements with conventional subsurface current meter moorings are also well known and are particularly severe in regions of strong, deep flow, such as in the Gulf Stream or Kuroshio. In such currents it is generally difficult to place current meters within several hundred meters of the surface and, even if this is done successfully, the data retrieved can often be seriously contaminated by mooring motion.

Recent engineering and field experiments with self-contained Acoustic Doppler Current Profilers (ADCPs) mounted in the upward-looking mode on subsurface moorings (Schott 1986; Schott and Johns 1987) have shown a promising new capability for measuring near-surface current profiles in such high-energy regions. In this application, ADCPs are moored several hundred meters below the surface in a low-to-moderate energy region underlying strongly sheared flow, and used to profile the overlying water column continuously. Aside from the obvious technical advantages in terms of mooring performance, this technique also offers several important scientific advantages. First, profiles of velocity are obtained over regions of complicated and rapidly varying vertical structure, rather than limited point measurements at a few depths. Second, even in the presence of strong mooring motion the ADCP provides continuous profiles up to near the surface (provided the acoustic range of the ADCP is not exceeded), and therefore allows reconstruction of time-series measurements at fixed, rather than variable, depths. The major disadvantage is that the Doppler measurement is inherently a noncontact measurement, so that information on water properties (e.g., temperature or conductivity) is not collected.

We report here on a brief field test of a 150 kHz ADCP deployed in the Gulf Stream off Cape Hatteras during November 1986 as part of a pilot experiment supported by the Office of Naval Research to test new sampling strategies for use in the SYNOP (Synoptic Ocean Prediction) observation program. The basic conclusion is that ADCPs moored in this upward-looking mode can be used to profile the upper water

Corresponding author address: Dr. William E. Johns, Rosenstiel School of Marine and Atmospheric Science, Division of Meteorology and Physical Oceanography, 4600 Rickenbacker Causeway, Miami, FL 33149-1098.

column accurately to within tens of meters of the surface for comparatively long periods of time, with an absolute accuracy of a few centimeters per second. In the first section we describe the measurement system and mooring configuration, including some details on a new streamlined buoy used to house the ADCP. Next, in section 3, we discuss the static and dynamic behavior of the ADCP flotation unit and some special considerations related to Doppler profiling in strong currents. Section 4 describes the ADCP velocity measurements and shows comparisons with data retrieved from an Aanderaa current meter 20 m below the ADCP, and with two Pegasus velocity profiles taken near the mooring site. Finally, in section 5, we summarize the results and discuss ways in which this technology can be used to address previously difficult scientific problems such as the near-surface eddy variability and momentum flux in high-speed baroclinic jets.

2. Measurement system

Acoustic Doppler Current Profilers* operate on the Doppler principle by transmitting short acoustic pulses along four vertically inclined beams and measuring the backscattered frequency shifts from small-scale particles and inhomogeneities within the overlying water column. Range-gated Doppler shifts are calculated along each of the four main beam paths and are proportional to the respective along-beam velocity components by

$$v_i = \frac{c\Delta f_i}{2f_t},$$

where Δf_i are the measured Doppler shifts along each beam, f_t is the transducer frequency, and c the sound speed at the level of the transducers. The factor of 2 arises because the ensonified water parcels act simultaneously as moving "observers" of the transmitted signal and moving "sources" for the backscattered signal. For each individual ping, the ADCP processor internally projects the along-beam Doppler shifts into earth-frame coordinates using the basic beam geometry, compass direction, and measurements from two-axis pendulum tilt sensors to account for deviations of the instrument axis from the vertical. The final output of the system is a scaled frequency shift in hertz along each of three (east, north, and vertical) coordinate axes, with scale factors varying according to acoustic frequency to yield values approximately equal to velocities in centimeters per second (e.g., for systems operating at nominal frequencies of 300, 150, and 75 kHz, the scale factors are 1, 2, and 4, respectively—see section 4 for a discussion of corrections which must be applied to these values). For most systems the velocity resolution is optional and may be selected at either 0.125 cm s^{-1} (for 0–256 cm s^{-1} total range) or 0.25 cm s^{-1} (for 0–512 cm s^{-1} total range).

The uncertainty in determining the along-beam Doppler shift for a single ping is a function primarily of the transducer frequency and the bin length (i.e., range increment); for the 150 kHz unit with a typical 8 m bin length it is approximately 15 cm s^{-1}. Thus, averages of a preselected number of pings, typically several hundred, are used to reduce the noise level to 1–2 cm s^{-1} and are stored as ensembles on a cassette tape (Schott 1986). For each ensemble the ADCP also stores the mean instrument heading, roll, and pitch angles, and with recent software modifications computes standard deviations of these quantities as a measure of the stability of the instrument orientation during a given ensemble.

The experiment consisted of two ADCPs housed within different flotation units on top of two separate moorings (see Fig. 1). One float was a standard 2000 lb-buoyancy syntactic foam sphere, while the second was a new low-buoyancy (~200 lb) streamlined float designed specifically for ADCP applications to minimize instrument tilt and vortex-shedding oscillations. A schematic of the streamlined float is shown in Fig. 2. Both ADCPs operated at 150 kHz, while the sphere-mounted ADCP had a 30° beam angle and the streamlined float-mounted ADCP had a 20° beam angle.

The configuration of the two moorings is shown in Fig. 1. The first mooring was placed near the mean location of the north wall of the Gulf Stream at 35°26′N, 73°59′W, in a total water depth of 2330 m, with the ADCP looking upward into strongly sheared flow. The second mooring, containing the streamlined float, was placed near the center of the Gulf Stream at

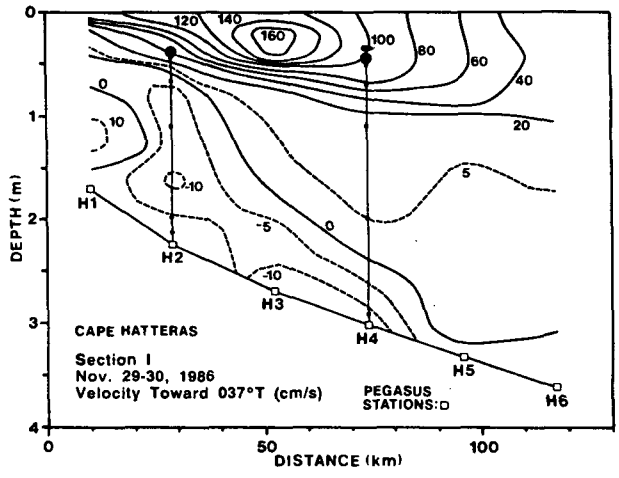

FIG. 1. Schematic of the mooring configuration off Cape Hatteras superimposed on a Pegasus velocity section taken 29–30 November 1986, near the end of the ADCP deployment. Current meters were placed at five levels on each of the moorings, indicated by dots. The velocity contours shown are in centimeters per second.

* The profilers are manufactured by R. D. Instruments, San Diego, California.

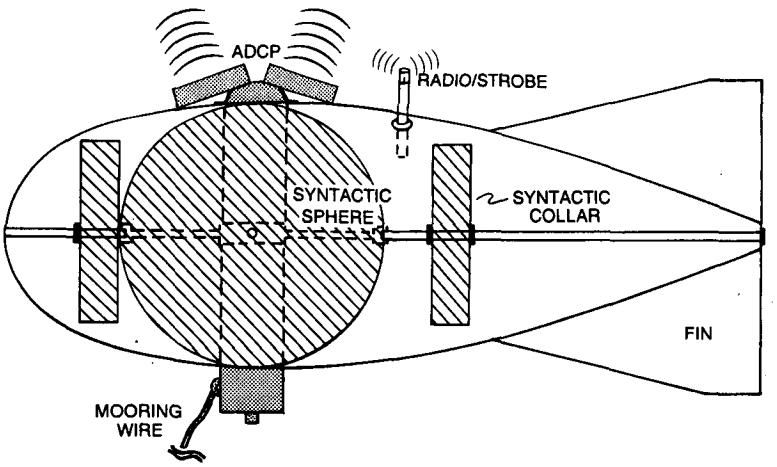

FIG. 2. Schematic diagram of the streamlined float. The outer hull is a freely flooding ¼ in. fiberglass shell built around a 32-inch syntactic foam sphere, in which the ADCP is integrally mounted. The aft section contains four stabilizing fins connected to a 36 in. diameter circular tail fin to provide structural support and added directional stability. Two 24 in. diameter syntactic foam disks are included within the shell as trim elements, which can be adjusted to provide a neutral buoyancy moment.

35°41′N, 74°22′W, slightly offshore of the mean surface velocity maximum (as indicated in Fig. 1), but near the point where the 100 cm s^{-1} isotach reaches its greatest depth. The total water depth at this mooring was 3080 m. Each mooring had Aanderaa current meters (ACMs) at five depths, including one near the top of each mooring directly below the ADCPs. Unfortunately, due to a tape recorder malfunction, no data were retrieved from the sphere-mounted ADCP, so that a comparison of the two systems, as originally intended, was not possible. In what follows we therefore restrict our discussion to the performance of the streamlined float and the accompanying Doppler velocity measurements at the offshore site, with only a few comments on the expected behavior of the sphere where a comparison seems appropriate.

During the experiment, vertical profiles of east, north, and vertical velocity and backscattered echo amplitude were recorded at nominal bin lengths of 8 m every 30 min. For each ensemble stored, 200 pings were averaged (at a rate of 1 s^{-1}), corresponding to a sampling interval of 3.3 min.

3. Float performance and sampling considerations

In optimizing the measurements from subsurface-moored ADCP systems, there are two key problems to be considered. The first is the effect of drag-induced tilt on the vertical range and precision of the velocity measurements. Under nominal (zero-tilt) operating conditions, there is always a near-surface layer of thickness $H(1 - \cos\theta)$, where H is the instrument depth and θ is the transducer beam angle, in which the Doppler velocities are biased due to interference from sidelobe returns traveling direct paths to the surface and back (Schott 1986). For example, for an ADCP with a 20° beam angle moored at 400 m depth (the case here), good data can only be obtained to within about 25 m of the surface. Any additional tilt increases the thickness of this biased zone rapidly (For a 20° tilt in the above example, e.g., with one beam therefore as much as 40° off vertical, good data can only be obtained to within approximately 100 m of the surface). Hence for near-surface applications it is essential to minimize instrument tilt due to hydrodynamic drag. A further problem is that during periods of even moderate inclination the ADCP processor must internally reassign range bins from the various beams so that Doppler currents are calculated from approximately the same depth. This, however, is not exact (there being no provision for interpolation) so that additional noise is introduced. For large inclinations greater than about 10°, the loss of symmetry in upward refraction of individual beams can also cause bias errors of a few percent in the Doppler currents, as well as additional errors in depth mapping. Of course, provided the Doppler data for each ping and each beam were stored, these secondary problems could all be corrected later based on knowledge of the sound speed profile although due to data storage limitations this is impractical for periods of more than a few hours.

The second major consideration is the effect of high-frequency mooring motion on the Doppler measurements themselves. At certain flow speeds, blunt bodies moored in a stream may oscillate as a result of periodic (Karman) vortex shedding in their wake. The oscillatory lift generated by the vortices can often be large; for example, the oscillatory lift on a circular cylinder has been measured at values approaching 40% of the total drag (Goldstein 1965, p. 421). Thus, for Doppler

measurements such vortex-induced oscillations could conceivably cause serious aliasing.

Considering first the static problem, the mean inclination of the top buoy on a subsurface mooring may be approximated simply by $\theta = \tan^{-1}(D/B)$, where D is the net hydrodynamic drag on the element and B is the net buoyancy of the element. This formula may be simply extended using an iterative procedure to calculate the expected static performance of an entire mooring, for a certain current profile, by stepping downward and including at each point the contributions to net drag and buoyancy from the sum of the overlying elements (Berteaux 1976). For most applications this simple procedure works quite well despite the fact that several factors are neglected, including tangential drag and the potential enhancement of drag due to oscillatory phenomena.

Less is known about the dynamic behavior of moorings. Modes of mooring oscillation range from high-frequency, transverse "strumming" of the mooring lines and components to lower-frequency longitudinal "elastic" oscillations of the entire mooring. For the present problem we are concerned primarily with the local response of a single buoy element attached to the mooring and free at its upper end. The basic transverse modes of oscillation of this system are those of a simple inverted (buoyancy) pendulum, with natural frequencies for symmetric bodies of approximately

$$f_0 = \frac{1}{2\pi}\left[\frac{(\rho_\omega - \rho)}{\rho}\frac{g}{l}\right]^{1/2}, \quad (1)$$

where ρ is the density of the float, ρ_ω the density of water, and l the effective length from the center of buoyancy to an assumed "rigid" attachment point. For high frequency "bobbing" oscillations this is essentially the point of coupling to the mooring, while for lower-frequency oscillations this may be expected to include progressively larger fractions of the length of underlying mooring line. The motion which is excited will depend on the frequency of forcing, while the magnitude of oscillation depends on the relative energy of the vortices (related to the bluntness of the body) versus the effects of viscous damping.

The streamlined float used in this experiment was modeled after traditional aerodynamic designs to reduce turbulent drag (hence also reducing the energy of wake vortices) and, through use of fins, to provide added directional stability. The range of Reynolds numbers expected, $\mathrm{Re} = UL/\nu$ (U and L are flow speed and float diameter, respectively; ν = kinematic viscosity), for flow speeds of 10–100 cm s^{-1} and a float dimension of 1 m, is approximately 10^5–10^6. Over the lower part of this range the drag coefficient for a body of revolution with a 3:1 aspect ratio similar to that of the float is found empirically to be about 0.1 (based on the frontal area), as compared, for example, to approximately 0.5 for a sphere (Hoerner 1965). At higher $\mathrm{Re} > 3$–4×10^5 these drag coefficients may be expected to drop appreciably upon transition to fully turbulent flow. Actual wind tunnel tests on scale models at Reynolds numbers of up to 3×10^5 were done to verify these values and to examine the effects of additional parasitic drag due to fins and/or exposed transducers. The net result was that the drag coefficient for the streamlined float was approximately 0.2, while for a similar-sized sphere carrying an ADCP it was approximately 0.6 (i.e., the comparable drag was reduced by a factor of about 3).

Figure 3 shows the mean pitch (fore–aft inclination) of the ADCP/streamlined float unit and its standard deviation as a function of current speed in the first Doppler bin. Over the speed range observed, the mean pitch varied from approximately 1° (at 60 cm s^{-1}) to 1.7° (at 100 cm s^{-1}). The mean roll (lateral inclination), also shown in Fig. 3, was approximately 0.5° and was virtually independent of speed, which suggests merely a small initial misalignment to the vertical. The expected drag on the float, using the quadratic drag formula

$$D = 1/2\rho_\omega c_D U^2 A,$$

where C_D is the drag coefficient (assumed for the moment to be a constant 0.2), U the speed, and A the exposed cross-sectional area of the float, would be approximately 4.5 lb in 60 cm s^{-1} of current and approximately 12 lb in 100 cm s^{-1} of current. Thus, with the net buoyancy of 200 lb, the inclinations would be $\tan^{-1}(D/B) \approx 1.3°$ and 3.4°, respectively. The fact that the mean pitch observed at 100 cm s^{-1} is about half that predicted is probably due to the restoring moment for nonzero inclinations provided by the horizontal fins, which in this case appears to become significant at speeds of approximately 80 cm s^{-1} and above, as indicated by the leveling off of the pitch versus speed curve there. This could also be partly due to a reduction

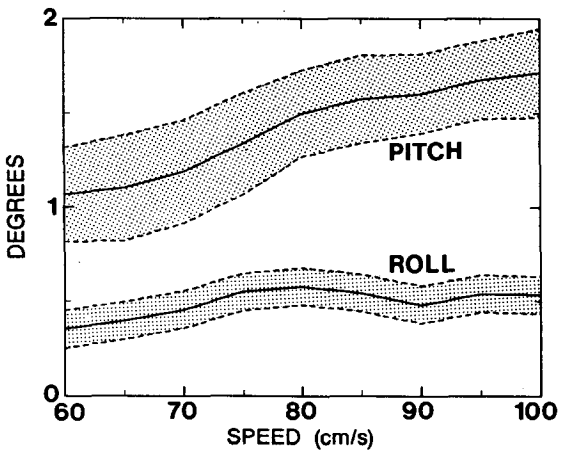

FIG. 3. Mean pitch (fore–aft inclination) and roll (side-to-side inclination) of the streamlined float-mounted ADCP, and associated standard deviations, vs current speed in the first Doppler bin.

in C_D beyond transition. For comparison, we note that in 100 cm s^{-1} of flow the expected tilt for the same 32-inch diameter sphere without the streamlined shell would be approximately 11°–12°, while for a 2000-lb (60-inch diameter) sphere it would be 4°–5°. Thus to achieve similar performance with spherical floats much larger buoyancies are required, although a tilt on the order of 5° (e.g., for the 2000-lb sphere) would seemingly be acceptable for most applications.

The dominant time dependent forcing is assumed to be due to vortex shedding behind the float which generates oscillating lift. Over a broad range of subcritical Reynolds numbers this vortex shedding is approximately periodic with frequency

$$f = \mathrm{St}(U/D) \tag{2}$$

where, as before, U and D are the velocity and float dimension scales and St is an empirically derived constant known as the Strouhal number. For Re = 10^4–(3×10^5) the Strouhal number for spheres increases smoothly from about 0.15 to 0.20, while at higher, supercritical Reynolds numbers the vortex shedding becomes more broadbanded and tends to be dominated by comparatively lower frequencies (Achenbach 1974). Willmarth and Enlow (1969) measured the oscillating lift on spheres in the supercritical Reynolds number range $4.5 \times 10^5 < \mathrm{Re} < 1.7 \times 10^6$ and found a fairly large root-mean-square lift coefficient of $C_L = 0.06$ (defined in the same way as C_D), which is a considerable fraction of the steady drag coefficient. No systematic measurements in the subcritical range have yet been made, although Scoggins' (1964) observations suggested that the oscillatory lift forces in this range are considerably smaller than in the supercritical range.

If for simplicity we assume that the Strouhal number is a constant 0.2, then for a float dimension of approximately 1 m and flow speeds of 10–100 cm s^{-1} the expected frequency of forcing ranges from 0.02 to 0.20 s^{-1}, corresponding to periods of oscillation of 5 to 50 s. By comparison, the highest natural frequency of oscillation of a moored syntactic foam buoy with density $\rho \sim 0.5$ and a distance from the center of buoyancy to the mooring attachment of 0.5 m is, according to (1), approximately 0.7 s^{-1}, corresponding to a period of 1.4 s. In reality, the minimum period of oscillation is probably longer due to added virtual mass effects (Sarpkaya 1975), effectively increasing the inertia of the float. For nonsymmetric or variable composition floats such as the streamlined float used here there are additional complications, in that the density contrast may be much greater or smaller and the moments of inertia in various planes may be different. A complete treatment of the problem is beyond the scope of this paper. The point simply is given the physical dimensions and composition of flotation materials commonly used in oceanographic moorings, the possibility of resonance at some flow speed (or even perhaps a broad range of speeds) is difficult to avoid. Although not done in this experiment, it would be useful at some point to mount accelerometer devices on subsurface floats, similar to those used on surface wave buoys, to measure the actual amplitudes and frequencies of such oscillations.

Some information on the high-frequency float behavior is provided by the ADCP tilt and heading sensors. Figure 3 shows the ensemble pitch and roll standard deviations about their mean values as a function of current speed. The pitch standard deviation was typically 0.2°–0.3°, appearing to decrease slightly with increasing speed, while the roll standard deviation was everywhere less than the least bit count of 0.1°. These small values have a negligible effect on the Doppler velocities.

One potential disadvantage of the streamlined float was that it might tend to "swim" back and forth in the current, thereby significantly aliasing the recorded Doppler shifts. This did not appear to be a problem, however. Figure 4 shows the ADCP compass heading (referenced to the forward pointing beam) versus current direction in the first Doppler bin. The directional stability of the float was quite good, with a standard deviation of only 1.4° between ADCP heading and current direction, roughly consistent with the uncertainty in determining the bin 1 velocity vector. Moreover, the heading standard deviation over individual 200 ping ensembles was everywhere less than the least bit count of 1°. Thus, both the static and dynamic performance of the float appear to be optimal for Doppler profiling.

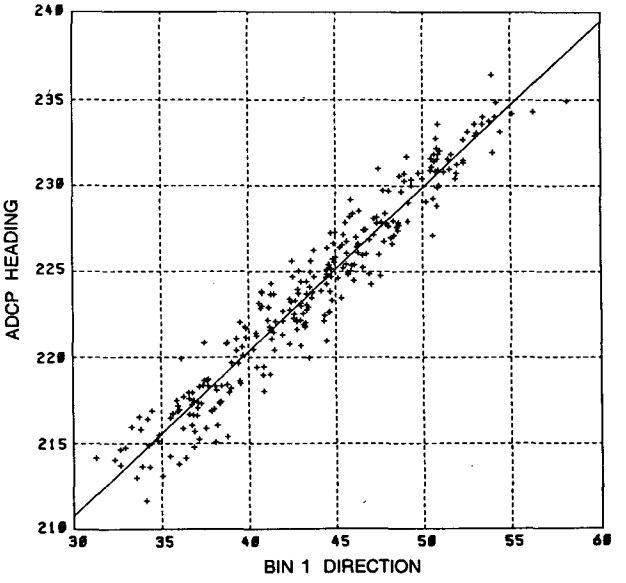

FIG. 4. Scatter plot of the ADCP heading (referenced to the forward pointing acoustic beam) vs current direction in the first Doppler bin. All directions are in true degrees. The rms deviation from a linear fit is 1.4 deg.

4. Velocity data

The postrecovery data processing consists of proper range-mapping of the time-gated Doppler signals, conversion of the approximate Doppler velocities to true velocities, and a final range-to-depth conversion based upon the actual depth of the ADCP at the time of each ensemble.

For any individual deployment, the true vertical range increment per bin will differ slightly from the nominal preselected value depending on the sound speed profile above the instrument. Hence for accurate depth mapping some ancillary measurement of the local sound speed profile is required. Figure 5 shows three XBT profiles taken at the ADCP mooring site during the beginning, middle, and end of the deployment, and the resulting sound speed profile based on the average of these temperature profiles and a mean TS relation. The mixed layer depth is 100–120 m, with the main thermocline (10°–15°C) located at approximately 500–700 m depth and an obvious 18°C water lens in the 250–450 m depth range. The sound speed varies from almost 1540 m s^{-1} near the surface to approximately 1523 m s^{-1} at the ADCP depth, with a mean value in the 0–400 m range of 1530 m s^{-1}. The true bin length, using a value of $c = 1530$ m s^{-1}, is 9.03 m, instead of the nominal 8 m. The large difference here is due to two factors; namely that the internal sound speed used in the ADCP is too low (Schott 1986), but also primarily because ADCPs manufactured with 20° beam angles currently use the same time-gating for the Doppler bins as for ADCPs built with 30° beam angles.

Under circumstances where the sound speed varies rapidly with depth over the profiling range it may also be necessary to include a range-dependent correction to the bin length. For example, in many regions of the ocean the sound speed increases by several percent over the upper part of the water column, and the bin length is stretched accordingly by an amount

$$\frac{l(z)}{l_0} = \frac{c(z)}{c_0}\left[\frac{\cos\left\{\sin^{-1}\left[\frac{c(z)}{c_0}\sin\theta_0\right]\right\}}{\cos\theta_0}\right] \sim 0.8 - 0.9 \times \frac{c(z)}{c_0}$$

where $l(z)$ and $c(z)$ are the bin length and sound speed, respectively, at a certain vertical range z; l_0 and c_0 the bin length and sound speed, respectively, at the instrument level; θ_0 the transducer beam angle; and the term in square brackets represents a small 10%–20% compensating effect due to ray refraction according to Snell's law, $\sin\theta/c$ = constant. In the present case the sound speed varies by only about 1%, and a constant bin length of 9.03 m was used throughout.

Figure 6 shows the mean echo amplitude profile over the deployment. The surface reflection of the slanted acoustic beams is evident as a strong peak in echo amplitude near 375 m range, corresponding to the mean ADCP depth (see Fig. 8). The first increase in echo amplitude occurs approximately 25–30 m deeper, as expected, due to surface returns from the vertically traveling sidelobes of the main beams. (Note that the surface expression shown here is somewhat broader than would be the case for any individual ensemble, due to the ~40 m ADCP depth variation over the deployment.)

The echo amplitude is still falling off fairly rapidly just prior to the surface returns, which suggests that a range capability for the 150 kHz ADCP approaching 400 m. Preliminary data from a 150 kHz ADCP

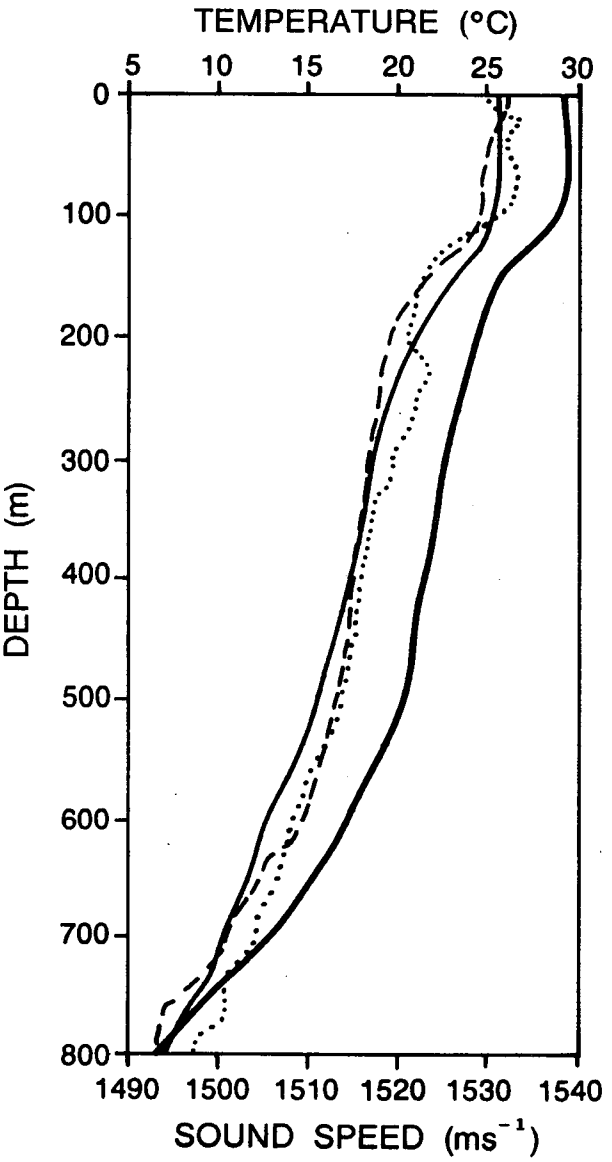

FIG. 5. Three XBT temperature profiles taken at the offshore ADCP site during the deployment (light lines), and the corresponding mean sound speed profile (bold solid line).

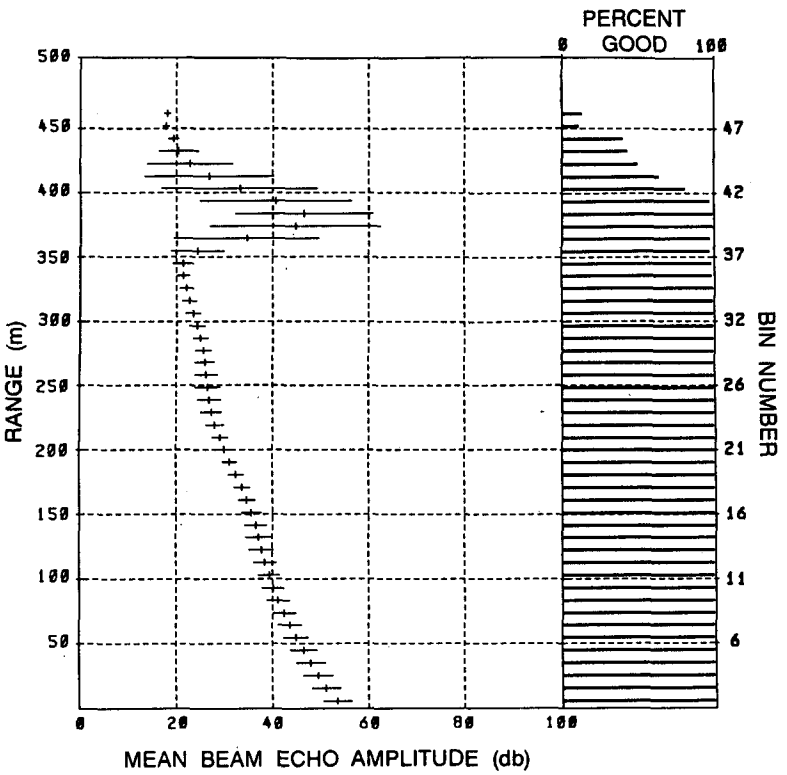

FIG. 6. Mean profiles of the backscattered echo amplitude, and the percentage of pings exceeding the noise threshold in each bin over the deployment.

moored in the Mediterranean Sea at 560 m depth (Schott, personal communication) indicate that good velocity data can in fact be obtained considerably beyond the point where the backscattered energy approaches the oceanic noise level, because the Doppler measurements are drawn from a narrower bandwidth than the recorded echo amplitude. This suggests that a profiling range of 400 m or greater for a 150 kHz unit might be attained on a fairly consistent basis.

Corrections to the Doppler velocity data are also necessary because the recorded values are simply scaled frequency shifts in hertz, and only correspond exactly to velocities in centimeters per second if the sound speed is 1536 m s^{-1}, since the actual transducer frequency is 153.6 kHz (Schott and Johns 1987). For the horizontal velocity components this correction is a constant multiplicative factor, $c_0/1536$ m s^{-1}, depending only on the sound speed at the transducer level, c_0. Variations in sound speed over the water column are exactly compensated by ray bending, again via Snell's law, so the projection of along-beam frequency shifts onto the horizontal is conserved, i.e., it is the same as if there were no sound speed variation (Schott and Johns 1987). Thus, for this deployment, with $c_0 = 1523$ m s^{-1}, the raw Doppler velocities were approximately 1% too high. For the vertical component the corresponding correction does depend on the sound speed profile, but is typically only 2%–3% and, for most applications, is therefore negligible compared to the noise level.

It should be emphasized here that the above simple corrections all depend implicitly on beam symmetry and are considerably more complex if the instrument axis deviates significantly from the vertical. Moreover, since the recorded data are ensembles of a large number of individual pings from four beams, such corrections would only be possible if the instrument tilt and heading remained essentially constant over any given ensemble interval.

Finally, velocity profiles are obtained by mapping the corrected range data into depth based on the actual depth of the ADCP transducers. Time series at constant depths are then created by linear interpolation of the velocity data in adjacent (depth-variable) bins. In general, the velocity data were extremely clean, with only part of one profile out of a total of 285 showing unreasonably large values, probably due to ship noise since it occurred shortly after the deployment.

Figure 7 shows contour plots of the horizontal velocity components projected onto mean downstream (045°T) and cross-stream (135°T) coordinate axes. The downstream speed shows a large variability (40–90 cm s^{-1}) over the upper 120–160 m, approximately the depth of the temperature mixed layer, with typically less variability below about 200 m. Occasionally large vertical shears occurred in the upper 100 m (e.g., near

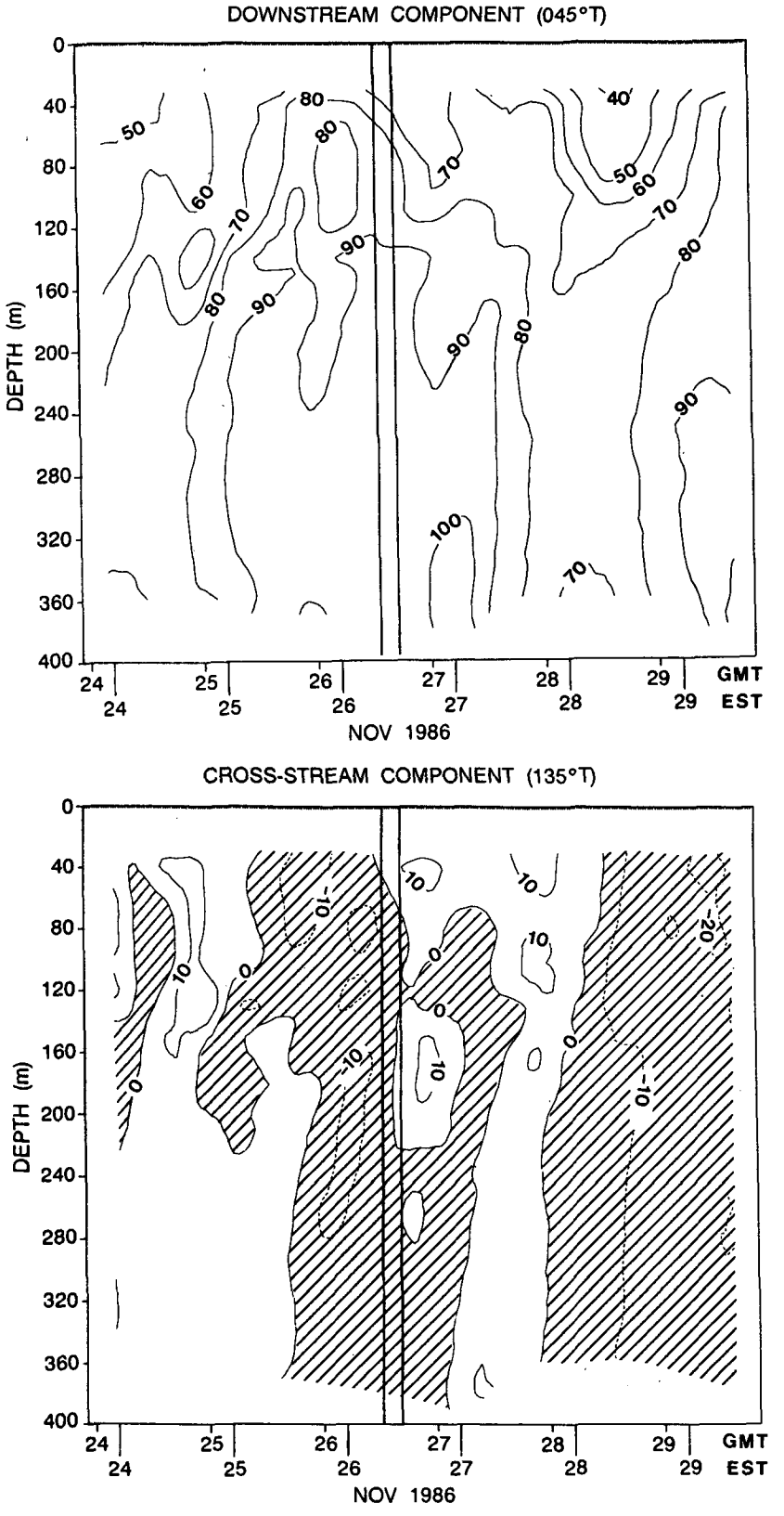

FIG. 7. (a) Depth vs time contour plot of the downstream component of velocity (projected along 045°T) over the ADCP deployment. The two vertical lines in the center of the figure indicate the times of Pegasus downcast and upcast comparison profiles (see Fig. 9). (b) As in (a) except for the cross-stream velocity component (along 135°T). Shaded regions indicate negative (northwest) velocities.

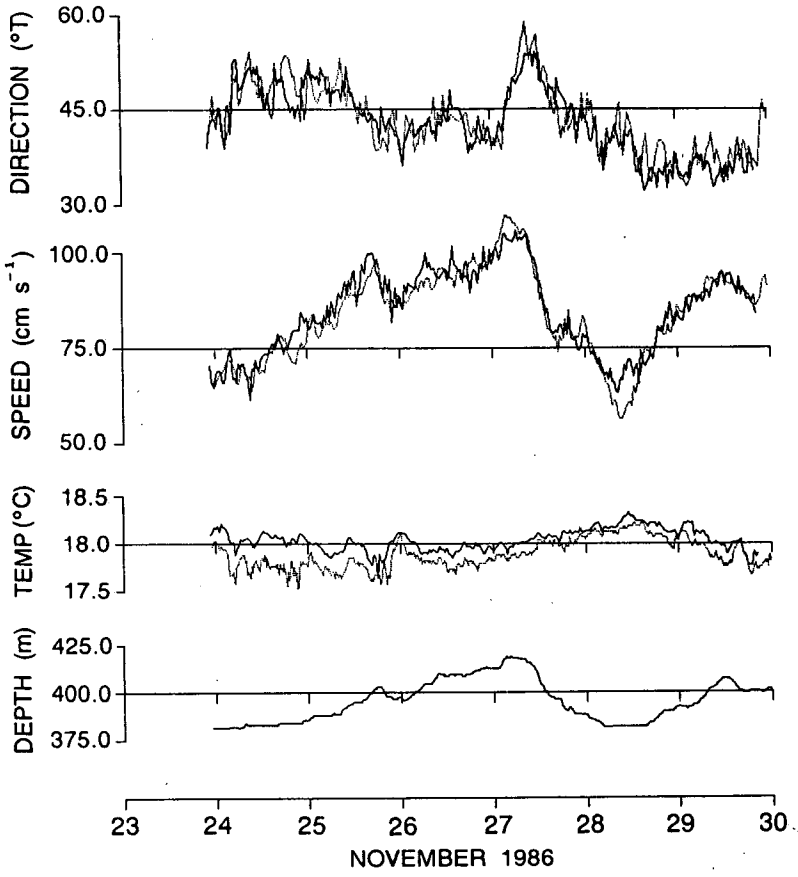

FIG. 8. Time-series comparison between the unfiltered ADCP speed and direction in the first Doppler bin, and ADCP temperature, with corresponding measurements from an Aanderaa current meter moored 20 m below the ADCP. The pressure record from the Aanderaa current meter is shown at the bottom.

28–29 November), whereas below the mixed layer the speed changes were predominantly barotropic. With few exceptions the speed reached a maximum value near the bottom of the profile, consistent with the subsurface velocity maximum usually found in this part of the Gulf Stream (cf. Halkin and Rossby 1985). The largest speed observed was 105 cm s^{-1}, occurring at the ADCP level (405 m) on 27 November. The cross-stream velocity component was typically 10 cm s^{-1} or less, and its changes were also fairly barotropic, indicating periodic direction changes but little large scale veering of the currents with depth.

Figure 8 shows the raw speed and direction comparison between the first Doppler bin of the ADCP and the ACM moored 20 m deeper. The measurements are highly correlated, with the directions generally agreeing to within a few degrees and speeds to within 5 cm s^{-1}. Due to random encoder problems the ACM direction data were rather spiky and had to be heavily edited, so that some of the apparent direction differences may be false. Significant speed differences occurred notably in two places, on 27 and 28 November, coinciding with the maximum and minimum flow speeds observed, respectively. In the first case the ADCP appeared to underestimate the speed, whereas in the second it appeared to overestimate the speed. These differences are probably attributable to the 20 m vertical separation between instruments, however, since as can be seen in Fig. 7a these two events correspond to times of weak negative and positive vertical shear, respectively, at the ADCP level, while over the rest of the record where there appears to be little or no vertical shear the agreement is better. Over the entire record the ADCP versus ACM correlation coefficients were 0.95 for speed and 0.86 for direction, with mean (rms) differences of 1.0 (3.7) cm s^{-1} and 0.5 (2.9) degrees, respectively.

Velocity profile comparisons were also available between the ADCP and a nearby Pegasus drop. Figure 9 shows the speed and direction profiles over the upper water column from both the downcast and upcast phases of a Pegasus drop taken within 1 n mi of the ADCP site on 1230 UTC to 1630 UTC 26 November (see also Fig. 7). The estimated maximum systematic

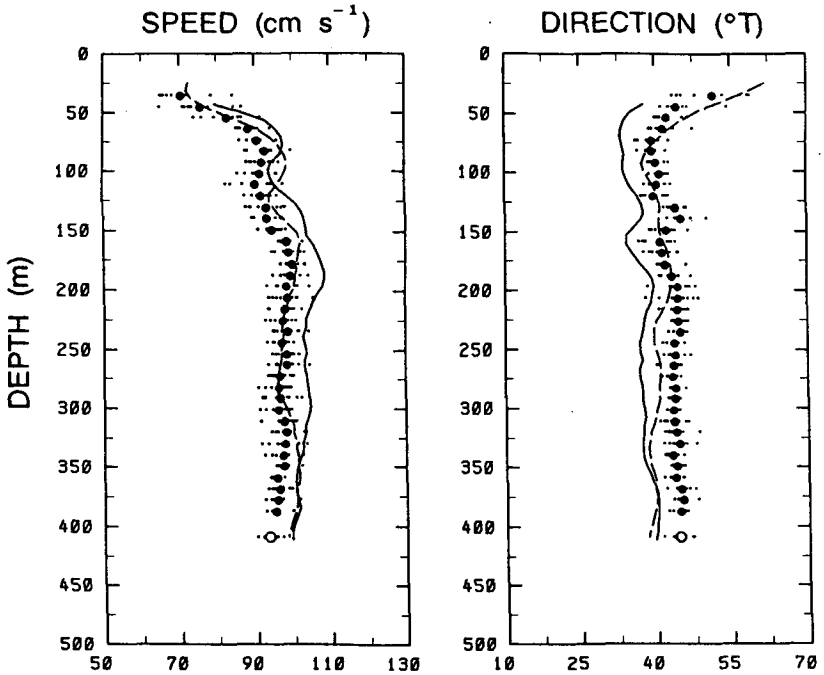

FIG. 9. Velocity profile comparisons between the ADCP and a Pegasus drop within 1 n mi of the ADCP site. The solid (dashed) lines show the PEGASUS downcast (upcast), separated in time by about four hours. The mean ADCP speed and direction profiles over this four-hour period are shown as solid dots, with the profile variability indicated by small dots. The open circles at the bottom of the profiles show the corresponding Aanderaa current meter speed and direction values.

errors in the Pegasus profiles are 2–3 cm s^{-1} for speed and 1° for direction, respectively (Leaman, personal communication). The accompanying ADCP profiles shown in Fig. 9 represent four-hour averages spanning the time of the complete Pegasus drop, with the variability about these mean profiles superimposed. For the downcast profile there are approximately constant offsets in both speed and direction, with the Pegasus-derived velocity being larger and veered counterclockwise relative to the ADCP velocity. By contrast, the upcast profile shows rather good agreement, with the Pegasus speed and direction profiles generally falling within the envelope of the ADCP profiles. An unambiguous quantitative comparison thus seems difficult, since the differences between the upcast and downcast profiles themselves are of the same order as the differences between either profile and the mean ADCP profile. Such upcast–downcast differences are not atypical of Pegasus drops taken near the high speed core of the Gulf Stream, due to the fact that the near surface profiles effectively sample water columns separated some 10–15 km in space in the alongstream direction and almost one-quarter of an inertial period in time. That these differences are real and not due to some instrument or processing problem is corroborated by the fact that below about 700 m, where the mean advective rates and inertial wave energies are much lower, the Pegasus profiles agree very closely. Qualitatively, at least, it is clear that the ADCP reproduces quite well the overall shape and small scale vertical structure in the PEGASUS profiles, and there is no apparent systematic ADCP bias with increasing vertical range. The ADCP speed and direction data agree well with the corresponding ACM data (shown at the bottom of the profiles), which show similar differences relative to the Pegasus profiles. In summary, based on the comparison with the ACM data, the ADCP velocity measurements appear to be accurate to within the theoretical 1–2 cm s^{-1} acoustical noise level.

Another potential application for ADCPs is in studying the diurnal vertical migration of zooplankton in the ocean and associated variations in backscattering strength due to vertical biomass redistributions. Figure 10 shows a depth versus time contour plot of the vertical velocity measured by the ADCP superimposed on the variations in backscattered echo amplitude. There is a clear diurnal cycle in the measured vertical velocity, with peak downward motions in the 250–350 m depth range occurring, on average, at 0620 EST, and peak upward motions at 1640 EST. By comparison, the times of local sunrise and sunset over the deployment were 0645–0650 EST and 1645–1650 EST, indicating a nice correspondence between the expected downward migration of scatterers prior to sunrise and upward mi-

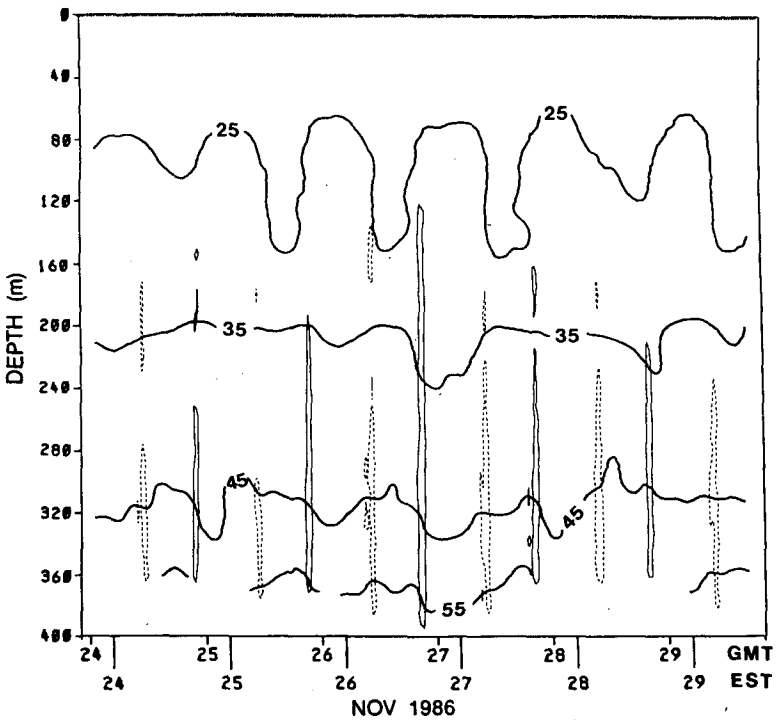

FIG. 10. Depth vs time contour plot of the backscattered echo amplitude (bold lines), superimposed on the measured ADCP vertical velocity. For vertical velocity the zero contour is suppressed and only values greater than or less than 2 cm s^{-1} are shown; the dashed contours represent negative (downward) velocities.

gration near sunset. [Note that for an acoustic frequency of 150 kHz the sound wavelength is roughly 1 cm, so that the primary scatterers should be micronekton in the 0.2 cm or larger equivalent spherical diameter class (Holliday, personal communication).] The vertical motion was strongest at approximately 350 m (at times exceeding 6 cm s^{-1}) and stopped rather abruptly at about 100 m depth. At approximately the 100 m depth level there is a corresponding modulation in the backscattering amplitude, with stronger echoes occurring during the night. At deeper levels there is no systematic antiphase variation, as one might expect, presumably because the primary scatterers were migrating back and forth from the region of the main thermocline located below the ADCP level. The single exception to this occurred on 27–28 November when there was a decrease in echo amplitude below approximately 200 m which followed an unusually strong upward migration. On several occasions, however, there were significant short-term fluctuations in backscattering amplitude apparently unrelated to vertical migration.

5. Discussion and conclusions

We report here on a brief field test of a moored ADCP system designed to measure velocity profiles in the upper layers of energetic ocean circulation regimes (e.g., the Gulf Stream) for extended durations. The results indicate that the ADCP velocity measurements are accurate to within the expected noise level of 1–2 cm s^{-1}, based on comparisons with an Aanderaa current meter moored 20 m beneath the ADCP. The profiling range of the 150 kHz ADCP is easily 350 m, with good data probably obtainable to 400 m or greater in most regions of the ocean.

Through the use of a new streamlined float designed to minimize drag-induced tilt, good velocity data were obtained to within 30 m of the surface from a mean depth of 375 m. This is an important precaution for near-surface ADCP applications, because 1) the thickness of the near-surface "shadow zone" due to acoustic sidelobe interference increases rapidly with increasing instrument tilt; and 2) for inclinations greater than a few degrees, additional noise is introduced in the computation of earth-frame Doppler velocities due to the truncated reassignment of range bins from various beams and, in certain cases, due to varying refractive effects on individual beams. For many applications a standard spherical top float with sufficiently large buoyancy should be adequate as a platform for ADCP measurements; large buoyancy is often necessary in any case to provide proper stiffness to deep ocean moorings. The streamlined float used here is a specialized tool that could be potentially useful in strong but comparatively shallow flows, where large buoyancy

is not needed to support a mooring, or also as a component that be could easily added to an existing mooring (as was done here) without dramatically increasing the tensional load and yet yielding good ADCP performance.

High-frequency buoy oscillations are also of some concern for acoustic Doppler measurements since aliasing could potentially occur if the amplitude-to-frequency ratio is large. For the streamlined float, the observed pitch, roll, and heading variations over approximately 3-min ensembles were small and had a negligible impact on the Doppler measurements. No comparable data were retrieved from a second, sphere-mounted ADCP, althoughn we anticipate that the oscillations of a sphere might be larger due to the greater oscillating lift generated on nonstreamlined shapes by wake vortices. For example, it is not inconceivable that an oscillation with a 0.5 m amplitude and period of, say, 10 s could occur, which would generate mean lateral speed oscillations of 20 cm s^{-1}. This is not as serious as it first appears, since if the phase of the oscillation is quasi-random this motion simply adds noise comparable to the acoustical noise ($\sim$15 cm s^{-1}) for a single ping. The real danger is that if the motion is approximately periodic and matches the ping rate, then a bias of this order can be introduced in the ensemble sample. Thus, since the shortest periods of oscillation expected are in the range of several seconds, to avoid this possibility occurring it is advisable to use the maximum ping rate consistent with the time it takes for surface reflections to clear the transducers; e.g., a ping rate of 1 s^{-1} is recommended unless the ADCP is moored deeper than approximately 700 m. As noted previously, little is known, at this time from direct measurements, how critical the high-frequency mooring motion problem might be; this bears further investigation.

A broad range of applications exists for buoy mounted ADCPs. One obvious use is in measuring the vertical current structure and near-surface Reynolds stresses in high-speed baroclinic flows that are difficult to sample using conventional moored technology, as was done here. Another use is in studying mixed-layer dynamics in the open ocean and near-surface velocity structure in high-vertical-mode regions, such as near the equator, where even current meter moorings with comparatively good vertical resolution can fail to resolve the true vertical structure. Coastal studies could also benefit from the use of ADCPs to obtain long-term records in regions of heavy fishing pressure, where conventional moorings could only be expected to survive for relatively short periods of time.

The vertical current measurement from ADCPs is potentially valuable for many applications, including studies of large-scale convection in regions of deep or intermediate water formation and, as briefly demonstrated here, for studies of biological scatterer migration (see also Schott and Johns 1987). With sufficient ping averaging, ADCPs may eventually be useful for measuring vertical motion in strong frontal regions such as the Gulf Stream, where vertical velocities of several millimeters per second have recently been observed (Rossby et al. 1985).

Acknowledgments. This work was supported by the Office of Naval Research under Contract N00014-87-K0008 to the University of Miami. I wish to thank R. Watts of U.R.I., J. Bane of U.N.C., and K. Leaman of RSMAS for their collaboration on this effort and for making the intercomparison data quickly available, and the captain and crew of the *R/V Endeavor* for helping to make this experiment successful. Comments on the manuscript by K. Leaman and F. Schott were helpful and greatly appreciated.

REFERENCES

Achenbach, E., 1974: Vortex shedding from spheres. *J. Fluid Mech.*, **62,** 209–221.

Berteaux, H. O., 1976: *Buoy Engineering.* Wiley & Sons.

Goldstein, S., 1965: *Modern Developments in Fluid Dynamics, Vol. 2.* Dover Publications.

Halkin, D., and T. Rossby, 1985: The structure and transport of the Gulf Stream at 73°W. *J. Phys. Oceanogr.*, **15,** 1439–1452.

Hoerner, S. F., 1965: *Fluid Dynamic Drag.* Published by author, New Jersey.

Rossby, T., A. S. Bower and P. T. Shaw, 1985: Particle pathways in the Gulf Stream. *Bull. Amer. Meteor. Soc.*, **66,** 1106–1110.

Sarpkaya, T., 1975: Forces on cylinders and spheres in a sinusoidally oscillating fluid. *J. Appl. Mech.*, **42,** 32–37.

Schott, F., 1986: Medium-range vertical acoustic Doppler current profiling from submerged buoys. *Deep-Sea Res.*, **33,** 1279–1292.

——, and W. E. Johns, 1987: Half-year long measurements with a buoy-mounted acoustic Doppler current profiler in the Somali Current. *J. Geophys. Res.*, **92,** 5169–5176.

Scoggins, J. R., 1964: Aerodynamics of spherical balloon wind sensors. *J. Geophys. Res.*, **69,** 591–598.

Willmarth, W. W., and R. L. Enlow, 1969: Aerodynamic lift and moment fluctuations of a sphere. *J. Fluid Mech.*, **36,** 417–432.